sciendo

TATRA MOUNTAINS
Mathematical Publications
DOI: 10.2478/tmmp-2020-0004
Tatra Mt. Math. Publ. **75** (2020), 49–62

FINITE VOLUME SCHEME FOR AMSS MODEL

Angela Handlovičová

Slovak University of Technology in Bratislava, Bratislava, SLOVAKIA

ABSTRACT. We propose a new finite volume numerical scheme for the approximation of the Affine Morphological Scale Space (AMSS) model. We derive the basic scheme and its iterative improvement. For both schemes, several numerical experiments using examples where the exact solution is known are presented. Then the numerical errors and experimental order of convergence of the proposed schemes is studied.

1. Introduction

From the mathematical point of view, the AMSS model can be described as a nonlinear degenerate parabolic equation with prescribed initial and boundary conditions. Then the goal of this study is to propose a new numerical scheme based on the finite volume methodology for this problem.

The AMSS model is one of the well-known models that arise in the area of image processing, with image filtering noisy images. There are several approaches to study these problems, from theoretical to numerical point of views. One can find more information e.g. in [1], [3], [4], [12], [16] and references therein. These problems are of high interest not only from mathematical point of view but from computer science and computer vision viewpoint as well. We can find much information for example in [10], [11] and [18]. The proposed model is based on the Mean Curvature operator and it is also known as Affine Morphological Scale Space (AMSS) model. In fact, it is a generalization of classical mean curvature model well-known in image processing. These models can be represented using highly nonlinear partial differential equations of parabolic type. That is why also the question of existence of a solution is worth of interest. Many important results in this field can be found for example in [2], [5], [7].

2010 Mathematics Subject Classification: Primary: 65M08; Secondary: 35K20.
Keywords: affine morphological scale space, image processing, finite volume scheme, experimental order of convergence.
This work was supported by VEGA 1/0728/15 and APVV-0522-15.

From numerical point of view various numerical schemes are derived especially for the mean curvature flow level set equation, for example [6], [8], [14], [15]. For the AMSS model one can find numerical scheme and its properties in [3]. This scheme represents Semi-Lagrangian approximation of this model where not only convergence of the numerical scheme but also numerical experiments which show the properties of obtained numerical approximation are presented.

The model can be written in the following form

$$u_t - |\nabla u| \left(\operatorname{div} \left(\frac{\nabla u}{|\nabla u|} \right) \right)^{\frac{1}{3}} = 0, \qquad \text{a.e.} \quad (t,x) \in (0,T) \times \Omega \tag{1}$$

with the initial condition

$$u(0,x) = u_0(x), \quad \text{a.e.} \qquad x \in \Omega, \tag{2}$$

and the boundary condition

$$u(t,x) = 0, \qquad \text{a.e.} \quad (t,x) \in (0,T) \times \partial\Omega, \tag{3}$$

where $\Omega \subset \Re^2$ and $\partial\Omega$ is its boundary. As the model is highly nonlinear and degenerate, we use the so-called Evans-Spruck [7] regularization to avoid zero values in denominator. Moreover, we use additional regularization, as in [8]. Thus our regularized problem is of the form

$$u_t - f(|\nabla u|) \left(\operatorname{div} \left(\frac{\nabla u}{f(|\nabla u|)} \right) \right)^{\frac{1}{3}} = 0, \qquad \text{a.e.} \quad (t,x) \in (0,T) \times \Omega, \tag{4}$$

where

$$f(s) = \min\{\sqrt{s^2 + a}, b\} \quad \text{for some parameters} \quad a > 0, \;\; b > 0. \tag{5}$$

The paper is organized as follows. In Section 2 we present the discretization tools. In Section 3 we propose numerical schemes. Numerical results are given in Section 4.

2. The finite volume tools

In order to describe the schemes, we now introduce some notations for the space discretization, see also [8].

Definition 2.1 (Space discretization)**.** Let Ω be a polyhedral open bounded connected subset of $\mathbb{R}^d$, with $d \in \mathbb{N}$, and $\partial\Omega = \overline{\Omega} \setminus \Omega$ its boundary. A discretization of Ω, denoted by $\mathcal{D}$, is defined as the triplet $\mathcal{D} = (\mathcal{M}, \mathcal{E}, \mathcal{P})$, where:

(1) $\mathcal{M}$ is a finite family of nonempty connected open disjoint subsets of Ω (the "control volumes") such that $\overline{\Omega} = \cup_{p \in \mathcal{M}} \overline{p}$. For any $p \in \mathcal{M}$, let $\partial p = \overline{p} \setminus p$ be the boundary of p; let $|p| > 0$ denote the measure of p and let h_p denote the diameter of p and $h_{\mathcal{D}}$ denote the maximum value of $(h_p)_{m \in \mathcal{M}}$.

(2) $\mathcal{E}$ is a finite family of disjoint subsets of $\overline{\Omega}$ (the "edges" of the mesh), such that, for all $\sigma \in \mathcal{E}$, σ is a nonempty open subset of a hyperplane of $\mathbb{R}^d$, whose $(d-1)$-dimensional measure $|\sigma|$ is strictly positive. We also assume that, for all $p \in \mathcal{M}$, there exists a subset $\mathcal{E}_p$ of $\mathcal{E}$ such that $\partial p = \cup_{\sigma \in \mathcal{E}_p} \overline{\sigma}$. For any $\sigma \in \mathcal{E}$, we denote by $\mathcal{M}_\sigma = \{p \in \mathcal{M}, \sigma \in \mathcal{E}_p\}$. We then assume that, for all $\sigma \in \mathcal{E}$, either $\mathcal{M}_\sigma$ has exactly one element and then $\sigma \subset \partial\Omega$ (the set of these interfaces, called boundary interfaces, is denoted by $\mathcal{E}_{\rm ext}$) or $\mathcal{M}_\sigma$ has exactly two elements (the set of these interfaces, called interior interfaces, is denoted by $\mathcal{E}_{\rm int}$). For all $\sigma \in \mathcal{E}$, we denote by x_σ the barycentre of σ. For all $p \in \mathcal{M}$ and $\sigma \in \mathcal{E}_p$, we denote by $\mathbf{n}_{p,\sigma}$ the unit vector normal to σ outward to p.

(3) $\mathcal{P}$ is a family of points of Ω indexed by $\mathcal{M}$, denoted by $\mathcal{P} = (x_p)_{p\in\mathcal{M}}$, such that for all $p \in \mathcal{M}$, $x_p \in p$ and p is assumed to be x_p-star-shaped, which means that for all $x \in p$, the inclusion $[x_p, x] \subset p$ holds. Denoting by $d_{p\sigma}$ the Euclidean distance between x_p and the hyperplane including σ, one assumes that $d_{p\sigma} > 0$. We then denote by $D_{p,\sigma}$ the cone with vertex x_p and basis σ.

(4) We make the important following assumption:

$$d_{p\sigma}\mathbf{n}_{p,\sigma} = x_\sigma - x_p, \quad \forall p \in \mathcal{M}, \quad \forall \sigma \in \mathcal{E}_p. \tag{6}$$

Remark 2.2. The preceding definition applies to triangular meshes if $d = 2$, with all angles acute, and to meshes build with orthogonal parallelepiped control volumes (rectangles if $d = 2$).

We denote

$$\theta_{\mathcal{D}} = \min_{p\in\mathcal{M}} \min_{\sigma\in\mathcal{E}_p} \frac{d_{p\sigma}}{h_p}. \tag{7}$$

Definition 2.3 (Space-time discretization)**.** Let Ω be a polyhedral open bounded connected subset of $\mathbb{R}^d$, with $d \in \mathbb{N}$ and let $T > 0$ be given. We say that $(\mathcal{D}, \tau)$ is a space-time discretization of $(0, T) \times \Omega$ if $\mathcal{D}$ is a space discretization of Ω in the sense of Definition 2.1 and if there exists $N_T \in \mathbb{N}$ with $T = (N_T+1)\tau$.

Let $(\mathcal{D}, \tau)$ be a space-time discretization of $\Omega \times (0, T)$. We define the set $H_{\mathcal{D}} \subset \mathbb{R}^{\mathcal{M}} \times \mathbb{R}^{\mathcal{E}}$ such that $u_\sigma = 0$ for all $\sigma \in \mathcal{E}_{\rm ext}$.

We define the following functions on $H_{\mathcal{D}}$

$$N_p(u)^2 = \frac{1}{|p|} \sum_{\sigma\in\mathcal{E}_p} \frac{|\sigma|}{d_{p\sigma}} (u_\sigma - u_p)^2, \quad \forall p \in \mathcal{M}, \quad \forall u \in H_{\mathcal{D}}. \tag{8}$$

Let us recall that

$$\|u\|_{1,\mathcal{D}}^2 = \sum_{p\in\mathcal{M}} |p| N_p(u)^2 \tag{9}$$

defines a norm on $H_{\mathcal{D}}$ (see [9]).

We then define the set $H_{\mathcal{D},\tau}$ of all $u = (u^{n+1})_{n=0,\dots,N_T}$ such that $u^{n+1} \in H_{\mathcal{D}}$ for all $n = 0, \dots, N_T$, and we set

$$\|u\|^2_{1,\mathcal{D},\tau} = \sum_{n=0}^{N_T} \tau \|u^{n+1}\|^2_{1,\mathcal{D}}, \quad \forall u \in H_{\mathcal{D},\tau}. \tag{10}$$

3. Numerical scheme

The idea to obtain numerical scheme is based on the finite volume methodology. Hence, we first rearrange and then integrate the equation (1) for arbitrary $p \in \mathcal{M}$ with the boundary ∂p and a unit outward normal $\mathbf{n_p}$. We obtain

$$\int_p \left(\frac{u_t}{f(|\nabla u|)} \right)^3 \mathrm{d}x + \int_{\partial p} \frac{\partial u}{\partial \mathbf{n_p}} \frac{1}{f(|\nabla u|)} \mathrm{d}s = 0. \tag{11}$$

Using the standard finite volume methodology we have

$$\left(\frac{(u_p^{n+1} - u_p^n)}{\tau \ f(N_p(u^n))} \right)^3 |p| - \frac{1}{f(N_p(u^n))} \sum_{\sigma \in \mathcal{E}_p} \frac{|\sigma|}{d_{p\sigma}} (u_\sigma^{n+1} - u_p^{n+1}) = 0,$$
$$\forall p \in \mathcal{M}, \ \ \forall n \in \mathbb{N}. \tag{12}$$

To obtain the linear scheme we can approximate the first term as

$$\frac{(u_p^{n+1} - u_p^n)}{\tau} \frac{(D_p^n)^2}{f(N_p(u^n))^3} |p|, \tag{13}$$

where D_p^n will be the approximation of the first derivative with respect to time in the previous time step. We now define the numerical scheme:

$$u_p^0 = \frac{1}{|p|} \int_p u_0(x) \mathrm{d}x, \quad \forall p \in \mathcal{M}, \tag{14}$$

$$u_\sigma^0 = \frac{1}{|\sigma|} \int_\sigma u_0(s) \mathrm{d}s, \quad \forall \sigma \in \mathcal{E}, \tag{15}$$

the boundary condition is fulfilled thanks to

$$u_\sigma^{n+1} = 0, \quad \forall \sigma \in \mathcal{E}_{\mathrm{ext}}, \quad \forall n \in \mathbb{N} \tag{16}$$

and

$$\frac{(u_p^{n+1} - u_p^n)}{\tau} \frac{(D_p^n)^2}{(f(N_p(u^n))^3} |p| - \frac{1}{f(N_p(u^n))} \sum_{\sigma \in \mathcal{E}_p} \frac{|\sigma|}{d_{p\sigma}} (u_\sigma^{n+1} - u_p^{n+1}) = 0,$$
$$\forall p \in \mathcal{M}, \ \forall n \in \mathbb{N}, \tag{17}$$

where the following relation is given for the interior edges [8]

$$\frac{u_\sigma^{n+1}-u_p^{n+1}}{f(N_p(u^n))\ d_{p\sigma}}+\frac{u_\sigma^{n+1}-u_q^{n+1}}{f(N_q(u^n))\ d_{q\sigma}}=0,\ \forall\sigma\in\mathcal{E}_{\rm int}\text{ with }\mathcal{M}_\sigma=\{p,q\},\ \forall n\in\mathbb{N}. \tag{18}$$

There are several possibilities to state the term D_p^n. We use the equation (11) and approximate it by the fully implicit scheme in the time step n. If we denote by $\tilde{D}_p^n$ the approximation of the first derivative with respect to time, we have analogously to (12)

$$\left(\frac{\tilde{D}_p^n}{f(N_p(u^n))}\right)^3|p|-\frac{1}{f(N_p(u^n))}\sum_{\sigma\in\mathcal{E}_p}\frac{|\sigma|}{d_{p\sigma}}(u_\sigma^n-u_p^n)=0,\quad \forall p\in\mathcal{M},\ \forall n\in\mathbb{N}. \tag{19}$$

From this equation we can compute the approximation $\tilde{D}_p^n$ immediately

$$\tilde{D}_p^n=\left(\frac{f(N_p(u^n))^2}{|p|}\sum_{\sigma\in\mathcal{E}_p}\frac{|\sigma|}{d_{p\sigma}}(u_\sigma^n-u_p^n)\right)^{\frac{1}{3}}, \tag{20}$$

and finally to avoid zero values of the approximation we define

$$D_n^p=\begin{cases}\max\{a_1,\tilde{D}_p^n\} & \text{if } \tilde{D}_p^n\geq 0\\ \max\{-a_1,\tilde{D}_p^n\} & \text{if } \tilde{D}_p^n\leq 0\end{cases}\qquad \forall p\in\mathcal{M},\ \forall n\in\mathbb{N}. \tag{21}$$

Now considering a family of values $(u_p^n)_{p\in\mathcal{M},n\in\mathbb{N}}$, given by (14), (3) and (15), (17), (18), we define (following [8]) the approximate solution $u_{\mathcal{D},\tau}$ in $\Omega\times\mathbb{R}_+$ by

$$u_{\mathcal{D},\tau}(x,0)=u_p^0,\quad u_{\mathcal{D},\tau}(x,t)=u_p^{n+1},\quad \text{for a.e. } x\in p,\ \forall t\in]n\tau,(n+1)\tau],\ \forall p\in\mathcal{M},\ \forall n\in\mathbb{N}. \tag{22}$$

Then we define $N_{\mathcal{D},\tau}$ and $\widetilde{N}_{\mathcal{D},\tau}$ by

$$N_{\mathcal{D},\tau}(x,t)=N_p(u^{n+1}),\quad \widetilde{N}_{\mathcal{D},\tau}(x,t)=N_p(u^n),\quad \text{for a.e. } x\in p,\ \text{for a.e. } t\in]n\tau,(n+1)\tau[,\ \forall p\in\mathcal{M},\ \forall n\in\mathbb{N}. \tag{23}$$

Finally, on $\Omega\subset\mathbb{R}^d$ and the time interval $(0,T)$ we define $G_{\mathcal{D},\tau}$ by

$$G_{\mathcal{D},\tau}(x,t)=d\frac{u_\sigma^{n+1}-u_p^{n+1}}{d_{p\sigma}}\mathbf{n}_{p\sigma},\quad \text{for a.e. } x\in D_{p\sigma},\ \text{for a.e. } t\in]n\tau,(n+1)\tau[,\ \forall p\in\mathcal{M},\ \forall\sigma\in\mathcal{E}_p,\ \forall n\in\mathbb{N}. \tag{24}$$

3.1. Semi-implicit scheme

First we can rearrange our numerical scheme in the following way: from (18) we can express

$$u_\sigma^{n+1} = \frac{u_p^{n+1} f(N_q(u^n))\ d_{p\sigma} + u_q^{n+1} f(N_p(u^n))\ d_{q\sigma}}{f(N_p(u^n))\ d_{p\sigma} + f(N_q(u^n))\ d_{q\sigma}},$$
$$\forall \sigma \in \mathcal{E}_{\rm int} \quad \text{with} \quad \mathcal{M}_\sigma = \{p, q\},\ \ \forall n \in \mathbb{N}. \quad (25)$$

Now substitute u_σ^{n+1} into (17) we obtain the scheme with unknowns u_p^{n+1}

$$\frac{(u_p^{n+1} - u_p^n)}{\tau} \frac{(D_p^n)^2}{(f(N_p(u^n))^3} |p| - \sum_{\sigma \in \mathcal{E}_p} \frac{(u_q^{n+1} - u_p^{n+1})|\sigma|}{f(N_p(u^n))\ d_{p\sigma} + f(N_q(u^n))\ d_{q\sigma}} = 0,$$
$$\forall p \in \mathcal{M},\ \ \forall n \in \mathbb{N}. \quad (26)$$

Now using the expression (21) for computing the term D_p^n for all $n \in \mathcal{M}$, and $n \in \mathbb{N}$, we obtain the basic numerical scheme for AMSS model.

3.2. Fully implicit (iterative) scheme

To achieve more accurate results, we can improve our numerical scheme using iterative method in which the proposed scheme will be the first step of iterations.

Suppose that we have the numerical solution at the nth time step. Then we denote

$$u_p^{n+1,0} = u_p^n, \quad \text{and} \quad D_p^{n,0} = D_p^n \quad \text{from (21)}.$$

For $k = 1, \dots n_{it}$ we compute $u_p^{n+1,k}$ from

$$\frac{(u_p^{n+1,k} - u_p^n)(D_p^{n,k-1})^2}{\tau(f(N_p(u^{n+1,k-1}))^3} |p| -$$
$$\sum_{\sigma \in \mathcal{E}_p} \frac{(u_q^{n+1,k} - u_p^{n+1,k})|\sigma|}{f(N_p(u^{n+1,k-1}))\ d_{p\sigma} + f(N_q(u^{n+1,k-1}))\ d_{q\sigma}} = 0,$$
$$\forall p \in \mathcal{M},\ \forall n \in \mathbb{N}, \quad (27)$$

and $u_\sigma^{n+1,k}$ from

$$u_\sigma^{n+1,k} = \frac{u_p^{n+1,k} f(N_p(u^{n+1,k-1}))\ d_{p\sigma} + u_q^{n+1,k} f(N_q(u^{n+1,k-1}))\ d_{q\sigma}}{f(N_p(u^{n+1,k-1}))\ d_{p\sigma} + f(N_q(u^{n+1,k-1}))\ d_{q\sigma}},$$
$$\forall \sigma \in \mathcal{E}_{\rm int} \text{ with } \mathcal{M}_\sigma = \{p, q\},\ \forall n \in \mathbb{N}. \quad (28)$$

We stop the iterations when either

$$\max_{\forall p \in \mathcal{M}} |u_p^{n+1,k} - u_p^{n+1,k+1}| \le \text{tol} \quad \text{or} \quad k + 1 = n_{it},$$

where tol is a prescribed tolerance.

4. Numerical experiments

In this section we present several examples to illustrate the numerical properties of the proposed finite volume (FV) schemes. We focus on the examples where the exact solution is known to study the errors of our numerical solution in various functional spaces and experimental convergence orders.

EXAMPLE 1. In this example, the exact solution of (1) with the homogeneous Neumann boundary condition is obtained from [3] and is of the form

$$u(x,y,t) = \max\left\{1 - (x^2+y^2)^{\frac{2}{3}} - \frac{4}{3}t, 0\right\}^2.$$

The initial condition is obtained from the exact solution for $t = 0$.

In this case, our domain Ω is a square $\Omega = [-2,2] \times [-2,2]$. The time interval is $I = [0, 0.32]$. One can see the shape of the solution and cuts of the exact solution for $y = 0$ in time $T = 0; 0.16; 0.32$ in Figure 1.

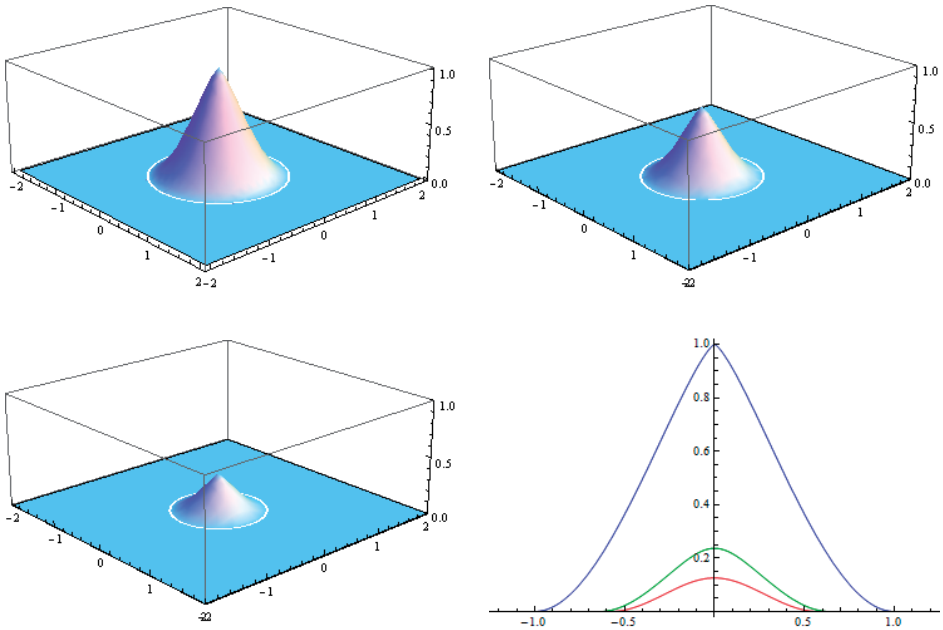

FIGURE 1. Example 1. The initial condition (top left) and the exact solution at time T=0.16 (top right), the exact solution at time T=0.32 (bottom left) and the shape of cuts ($y = 0$;) for initial condition (blue) and exact solution at time T=0.16 (green), T=0.32 (red).

In tables below, we present the errors obtained by the numerical schemes on various examples, the experimental order of convergence (EOC) in several functional spaces and CPU times (in seconds) for the methods. The considered errors are

$$E_2 = \|u_{\mathcal{D},\tau} - \bar{u}\|_{L^2(\Omega\times(0,T))},$$

and

$$EG_2 = \|G_{\mathcal{D},\tau} - \nabla\bar{u}\|_{L^2(\Omega\times(0,T))^2},$$

where numerical functions are defined in (22) and (24),

$$\bar{u}(x,t) = u(x_p,t_n) \qquad \text{for } x \in p \qquad \text{and} \qquad t \in < t_{n-1}, t_n >,$$
$$\nabla\bar{u}(x,t) = \nabla u(x_p,t_n) \qquad \text{for } x \in p \qquad \text{and} \qquad t \in < t_{n-1}, t_n > .$$

For this example we present results computed by the semi-implicit scheme and the iterative fully implicit scheme as well. For all experiments we use parameter of the scheme $b = 10^8$. Further by N we denote the number of finite volumes along one side of the domain Ω. We use the relation $\tau = h^2$ where $h = |\sigma| > 0$ is the measure of the edge for finite volume (we have uniform mesh). We use the SOR iterative method for solving the linear algebraic system with parameter $\alpha = 1.3$ and tolerance $tol = 10^{-8}$.

For the semi-implicit scheme we present two experiments. For the first one we choose $a_1 = a = 10^{-14}$ parameters of the scheme and the results can be seen in Table 1.

TABLE 1. Example 1, error reports, EOCs and CPU times for the semi-implicit FV scheme with $a_1 = a = 10^{-14}$

N	τ	E_2	EOC	EG_2	EOC	CPU
10	1.6e-01	2.83e-02	—	1.49e-01	—	1.70 e-02
20	4.0e-02	1.91e-02	0.568	1.15e-01	0.374	1.33 e-01
40	1.0e-02	9.73e-03	0.974	7.97e-02	0.530	8.93 e-01
80	2.50e-03	3.77-03	1.369	4.30e-02	0.890	8.26 e-00
160	6.25e-04	1.25e-03	1.593	2.31e-02	0.900	1.76e+02
320	1.5625e-04	3.92e-04	1.673	1.37e-02	0.756	1.84e+03

For the second experiment we choose $a_1 = 10^{-14}$ and $a = h^4$. The results are summarized in Table 2. As one can see the results are very similar for both experiments concerning EOC. Errors E_2 are little bit better in the first experiment. The similar results were obtained for the numerical solution of the mean curvature level set equation in [8].

TABLE 2. Example 1, error reports, EOCs and CPU times for the semi-implicit FV scheme with $a_1 = 10^{-14}$ and $a = h^4$.

N	τ	E_2	EOC	EG_2	EOC	CPU
10	1.6e-01	1.51e-01	—	1.48e-01	—	0.0e-00
20	4.0e-02	2.96e-02	2.354	1.17e-01	0.341	1.7e-01
40	1.0e-02	1.13e-02	1.384	7.88e-02	0.569	3.1e-01
80	2.5e-03	4.05e-03	1.483	4.23e-02	0.896	4.0e+00
160	6.25e-04	1.30e-03	1.636	2.29e-02	0.888	6.8e+01
320	1.5625e-04	4.04e-04	1.690	1.36e-02	0.748	1.0e+03

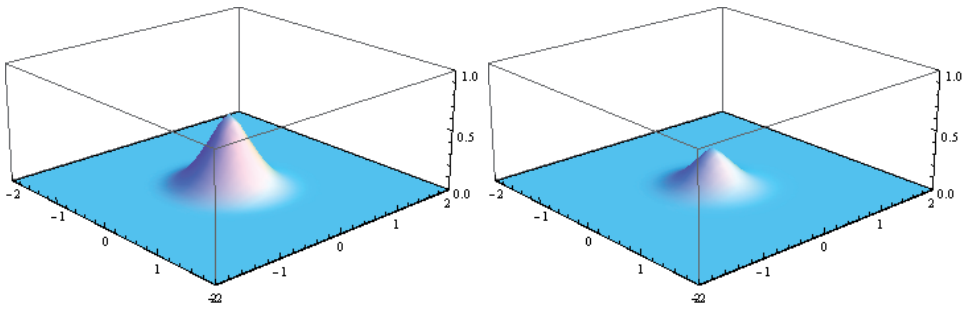

FIGURE 2. Example 1, Semi-implicit method, numerical solution at time T=0.16 (left) and at time T=0.32 (right).

The shape of the numerical solution obtained using the semi-implicit scheme can be seen in Figure 2, for $N = 40$ in visualization results.

For the fully implicit iterative scheme we present again two experiments with the same parameters as for the semi-implicit scheme. The results for parameters $a_1 = a = 10^{-14}$ are in Table 3 and for parameters $a_1 = 10^{-14}$ and $a = h^4$ in Table 4.

The shape of the numerical solution obtained using the iterative fully implicit scheme can be seen in Figure 3. From this first example one can see that the fully implicit iterative scheme is more accurate but it is much more time-consuming because in every time step we need, in average, about 40 nonlinear iterations.

TABLE 3. Example 1, error reports, EOCs and CPU times for the iterative fully implicit FV scheme with $a_1 = a = 10^{-14}$.

n	τ	E_2	EOC	EG_2	EOC	CPU
10	1.6e-01	3.75e-02	—	8.01e-02	—	7.8e-02
20	4.0e-02	1.20e-02	0.906	8.04e-02	-0.007	7.2e-01
40	1.0e-02	3.50e-03	2.517	5.20e-02	0.600	7.9e00
80	2.5e-03	1.12e-03	1.608	3.44e-02	0.595	1.4e+02
160	6.25e-04	4.48e-04	1.355	2.38e-02	0.536	1.6e+03
320	1.5625e-04	2.02e-04	1.145	1.68e-02	0.500	2.6e+04

TABLE 4. Example 1, error reports, EOCs and CPU times for the fully implicit iterative FV scheme with $a_1 = 10^{-14}$ and $a = h^4$.

n	τ	E_2	EOC	EG_2	EOC	CPU
10	1.6e-01	1.01e-01	—	1.78e-01	—	8.1e-02
20	4.0e-02	2.32e-02	2.127	9.45e-02	0.913	4.4e-01
40	1.0e-02	5.93e-03	1.966	5.55e-02	0.769	6.3e-00
80	2.50e-03	1.66-03	1.832	3.52e-02	0.659	9.39e+01
160	6.25e-04	5.41e-04	1.621	2.38e-02	0.559	1.25e+03
320	1.5625e-04	2.16e-04	1.323	1.68e-02	0.505	2.6e+04

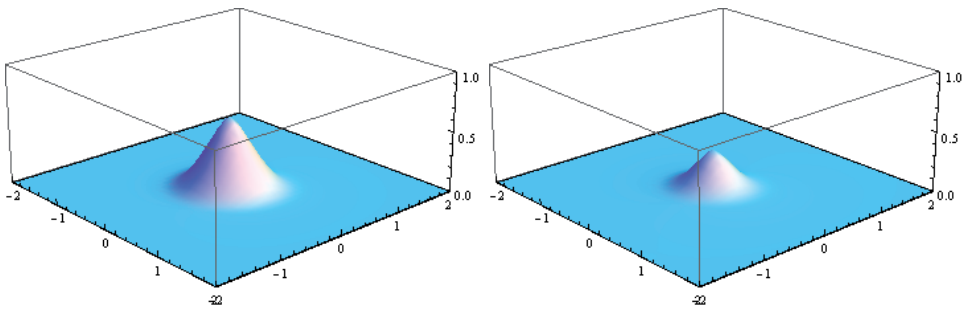

FIGURE 3. Example 1, Iterative fully implicit method, numerical solution at time T=0.16 (left) and at time T=0.32 (right)

EXAMPLE 2. In this example we compare the evolution of a closed curve for the cases when we know the exact solution [12]. This curve represents the zero level set of our numerical solution. The numerical zero level set curve can be detected using the interpolation method. That means our numerical zero level set is given by a certain number of interpolating points depending on the discretization of computational domain and, of course, on the time step, because the curve is shortening during the time. For the exact solution we define points on the curve uniformly redistributed. The number of such points, P, depends on the discretization by the relation $P = \frac{2\pi}{h}$, where h is a mesh discretization parameter.

In this case for comparison of two closed curves given by two discrete sets of points, we have used the mean Hausdorff distance [13] given by the following formula

$$\bar{d}_h(A,B) = \frac{\bar{\delta}_h(A,B) + \bar{\delta}_h(B,A)}{2},$$

where

$$\bar{\delta}_h(A,B) = \frac{1}{n}\sum_{i=1}^{n} \min_{b\in B} d(a_i,b) \quad \text{and} \quad \bar{\delta}_h(B,A) = \frac{1}{m}\sum_{i=1}^{m} \min_{a\in A} d(a,b_i), \tag{29}$$

where $d(a,b)$ is the Euclidean distance of two points a and b and

$$A = \{a_1,\dots,a_n\} \quad \text{and} \quad B = \{b_1,\dots,b_m\}.$$

We performed two numerical experiments, evolution of the circle and evolution of the ellipse. The exact solutions of $X(u,t)$ are given by formulas ($t \geq 0$ is the time variable and $u \in < 0,1 >$ is the parametrization of a curve):

(1) Circle with initial radius $r > 0$:

$$X(u,t) = \left(1 - \frac{4}{3} r^{-\frac{4}{3}} t\right)^{\frac{3}{4}} \big(\cos(2\pi u), \sin(2\pi u)\big)$$
$$\text{with life-span of a solution is} \quad T_{\max} = \frac{3}{4} r^{\frac{4}{3}} \tag{30}$$

(2) Ellipse with initial data $a > 0, b > 0$:

$$X(u,t) = \left(1 - \frac{4}{3} (ab)^{-\frac{2}{3}} t\right)^{\frac{3}{4}} \big(a\cos(2\pi u), b\sin(2\pi u)\big)$$
$$\text{with life-span of a solution is} \quad T_{\max} = \frac{3}{4}(ab)^{\frac{2}{3}}. \tag{31}$$

Evolution of circle. This experiment is devoted to the evolving of a circle given by (30) with initial radius $r = 1$. In Table 5 we present the mean Hausdorff distances for the exact curve and the curve obtained by linear interpolation of the zero level set for the numerical solution of the AMSS model. The computational domain Ω is a square $\Omega = [-1.25, 1.25] \times [-1.25, 1.25]$.

We use the iterative fully implicit scheme with the following parameters: $a_1 = 10^{-14}$, $a = 10^{-12}$ and tolerance $\mathrm{tol} = 10^{-6}$. We present the results obtained at the time $t = 0.25$, the mean Hausdorff distance is denoted by $\bar{d}_h(0.25)$ and at the time $t = 0.5$ by $\bar{d}_h(0.5)$. Computed Hausdorff distances are in Table 5. Again by N we denote the number of finite volumes along one side of the domain Ω. We use the relation $\tau = h^2$, where $h = |\sigma| > 0$ is the measure of the edge for finite volume.

TABLE 5. Example 2, evolving circle Hausdorff distances at time $t = 0.25$ and $t = 0.5$, EOCs for the fully implicit iterative FV scheme.

N	τ	$\bar{d}_h(0.25)$	EOC	$\bar{d}_h(0.5)$	EOC
10	6.25e-02	9.433e-02	—	1.7245e-01	—
20	1.5625e-02	2.050e-02	2.202	4.1127e-02	2.068
40	3.90625e-03	2.790e-03	2.877	8.156e-03	2.334
80	9.76563e-04	3.651e-04	2.934	1.090e-03	2.904
160	2.44141e-04	1.520e-04	1.265	2.512e-04	2.119

Evolution of ellipse. This experiment is devoted to the evolution of ellipse given by (31) with initial parameters $a = 1.0$, and $b = 0.5$. In Table 6 we present the mean Hausdorff distances for the exact ellipse and the curve obtained by interpolation of the zero level se tof the numerical solution of AMSS model. $\Omega = [-1.25, 1.25] \times [-1.25, 1.25]$. We use iterative scheme with the following parameters: $a_1 = 10^{-14}$, $a = 10^{-12}$ and tolerance $tol = 10^{-6}$. We present the result obtained for time $t = 0.125$ and the Hausdorff distance we denote in the table by $\bar{d}_h(0.125)$ and for the time $t = 0.25$ we denote the computed Hausdorff distance by $\bar{d}_h(0.25)$.

TABLE 6. Example 2, evolving ellipse Hausdorff distances at time $t = 0.125$ and $t = 0.25$, EOCs for the fully implicit iterative FV scheme.

N	τ	$\bar{d}_h(0.125)$	EOC	$\bar{d}_h(0.25)$	EOC
10	6.25e-02	1.741e-02	—	6.330e-02	—
20	1.5625e-02	9.760e-03	0.834	1.921e-02	1.720
40	3.90625e-03	3.115e-03	1.648	2.577e-03	2.898
80	9.76563e-04	6.972e-04	2.160	8.321e-04	1.631
160	2.44141e-04	2.301e-04	1.600	2.622e-04	1.667

5. Conclusion

We studied the regularized AMSS model from the numerical point of view. We presented two numerical schemes based on the finite volume methodology. On several experiments we performed the error measurements, and we presented the experimental order of convergence for the examples where the exact solution is known. Other experiments concerning image filtering can be found in [17]. In the future, we want to propose and study the nonlinear Crank-Nicolson scheme, show the numerical Affine Invariance Property of proposed scheme, and prove the stability estimates and convergence results.

REFERENCES

[1] ALVAREZ, L.—GUICHARD, F.—LIONS, P.-L.—MOREL, J.-M.: *Axioms and fundamental equations of image processing*, Arch. Rational Mech. Anal. **123** (1993), 199–257.

[2] BARLES, G.—SOUGANIDIS, P. E.: *Convergence of approximation schemes for fully nonlinear second order equations*, Asymptotic Anal. **4** (1991), 271–283.

[3] CARLINI, E.—FERRETTI, R.: *A Semi-Lagrangian approximation for the AMSS model of image processing*, Appl. Numer. Math. **73**, (2013), 16–32.

[4] CATTÉ, F.—LIONS, P.-L.—MOREL, J.-M.—COLL, T.: *Image selective smoothing and edge detection by nonlinear diffusion*, SIAM J. Numer. Anal. **29** (1992), 182–193.

[5] CHEN, Y.-G.—GIGA, Y.—GOTO, S.: *Uniqueness and existence of viscosity solutions ofgeneralized mean curvature flow equations*, J. Differ. Geom. **33** (1991), 749–786.

[6] DECKELNICK, K.—DZIUK, G.: *Convergence of numerical schemes for the approximation of level set solutions to mean curvature flow*, In:*Numerical methods for viscosity solutions and applications (Heraklion, 1999)*. (Maurizio Falcone, ed. et al.), Ser. Adv. Math. Appl. Sci. Vol. 59, World Sci. Publ., River Edge, NJ, 2001, pp. 77–93.

[7] EVANS, L.—SPRUCK, J.: *Motion of level sets by mean curvature. I*, J. Differ. Geom. **33** (1991), 635–681.

[8] EYMARD, R.—HANDLOVIČOVÁ, A. H.—MIKULA, K.: *Study of a finite volume scheme for regularized mean curvature flow level set equation*, J. Numer. Anal. **31** (2011), no. 3, 813–846.

[9] EYMARD, R.—GALLOUËT, T.—HERBIN, R.: *Discretization of heterogeneous and anisotropic diffusion problems on general nonconforming meshes. SUSHI: A scheme using stabilization and hybrid interfaces*, IMA J. Numer. Anal. **30** (2010), no. 4, 1009–1043

[10] LINDEBERG, T.: *Scale-space theory in computer vision*. In:*The Kluwer International Series in Engineering and Computer Science. Vol. 256*, Kluwer Academic Publishers, Dordrecht, 1993.

[11] LINDEBERG, T.: *Generalized Gaussian scale-space Axiomatics comprising linear scale-space, affine scale-space and spatio-temporal scale-space*, J. Math. Imaging Vision **40** (2011), no. 1, 36–81.

[12] MIKULA, K.—ŠEVČOVIČ, D.: *Solution of nonlinearly curvature driven evolution of plane curves*, Appl. Numer. Math. **31** (1999), 191–207.

[13] MIKULA, K.—URBÁN, J.—KOLLÁR, M.—AMBROZ, M.—JAROLÍNEK, J.—ŠIBÍK, I. —ŠIBÍKOVÁ, M.: *An automated segmentation of natura 2000 habitats from sentinel-2 optical data*, Discrete and Continuous Dynamicla Systems Ser. S. (to appear)

[14] OSHER, S.—FEDKIW, R.: *Level set methods and dynamic implicit surfaces*. In: *Applied Mathematical Sciences, Vol. 153*, Springer-Verlag, New York, NY, 2003.

[15] OSHER, S.—SETHIAN, J. A.: *Fronts propagating with curvature-dependent speed: Algorithms based on Hamilton-Jacobi formulations*, J. Comput. Phys. **79** (1988), 12–49.

[16] PERONA, P.—MALIK, J.: *Scale-space and edge detection using anisotropic diffusion*, IEEE Transactions on Pattern Analysis and Machine Intelligence **12** (1990), 629–639.

[17] POLAKOVIČOVÁ, Z.: *Numerical Scheme for AMSS model for image processing*. Diploma Thesis Dept. of Math and Descr. Geom. Fac. of Civil Engineering STU Bratislava, (2018). (In Slovak)

[18] SAPIRO, G.—TANNENBAUM, A.: *Affine invariant scale-space*, Internat. J. Comput. Vision **11** (1993), 25–44.

Received July 11, 2019

Department of Mathematics and Descriptive Geometry
Faculty of Civil Engineering
Slovak University of Technology in Bratislava
Radlinského 11
SK–810-05 Bratislava
SLOVAKIA
E-mail: angela.handlovicova@stuba.sk